iScience

CellPress
OPEN ACCESS

Review

Silk-based bioinspired structural and functional materials

Zongpu Xu,[1,2] Weiwei Gao,[3,*] and Hao Bai[4,*]

SUMMARY

Natural biological materials provide a rich source of inspiration for building high-performance materials with extensive applications. By mimicking their chemical compositions and hierarchical architectures, the past decades have witnessed the rapid development of bioinspired materials. As a very promising biosourced raw material, silk is drawing increasing attention due to excellent mechanical properties, favorable versatility, and good biocompatibility. In this review, we provide an overview of the recent progress in silk-based bioinspired structural and functional materials. We first give a brief introduction of silk, covering its sources, features, extraction, and forms. We then summarize the preparation and application of silk-based materials mimicking four typical biological materials including bone, nacre, skin, and polar bear hair. Finally, we discuss the current challenges and future prospects of this field.

INTRODUCTION

Many biological materials, such as bone, nacre, bamboo, spider silk, polar bear hair, and skin, possess remarkable mechanical properties, as well as some unique functions, generally originating from their multi-scale structures (Eder et al., 2018; Meyers et al., 2013; Wegst et al., 2015). Learning from these natural examples will stimulate the development of high-performance structural and functional materials, due to their great demands in various important fields, including aircraft technology, automobile manufacturing, electronic sensing, tissue engineering, and personal thermal management (Bhattacharjee et al., 2017; Chortos and Bao, 2014; Cui et al., 2018; Guan et al., 2020; Li et al., 2020a; Mao et al., 2021; Pan et al., 2021). During the past decades, significant progress has been achieved in bioinspired materials. A series of methodologies, from component selection, biomimetic structure design, fabrication procedure, to application demonstration, have been intensively explored. For example, mimicking natural nacre's elegant "brick-and-mortar" architectures, bulk synthetic nacre could be successfully constructed by infiltrating epoxy resin into a predesigned nanomaterial framework, which exhibited excellent strength and toughness comparable or even superior to natural nacre (Bai et al., 2016; Du et al., 2019a; Han et al., 2019; Zhao et al., 2020).

It is also worth noting that high-performance biological materials typically consist of components like proteins, polysaccharides, or minerals, which are biodegradable and sustainable (Mohanty et al., 2018; Wegst et al., 2015). This has become increasingly important as the petroleum-based polymers are difficult to biodegrade, leading to rapidly growing pollution problems worldwide (Geyer et al., 2017; Jambeck et al., 2015). Therefore, in part or in whole, using biopolymers as building blocks to construct bioinspired materials emerge as an attracting alternative (Li et al., 2021). To this extent, many biopolymers including collagen, silk, cellulose, chitin, chitosan, and alginate have been investigated to develop composites with biomimetic structures. Among them, silk stands out for its excellent mechanical properties, favorable versatility, and good biocompatibility (Holland et al., 2019; Melke et al., 2016; Omenetto and Kaplan, 2010; Shao and Vollrath, 2002; Tao et al., 2012; Xu et al., 2019), making it a promising raw material for building multiple biomimetic systems.

Recently, silk-based bioinspired structural and functional materials have drawn increasing attention. In this work, we overview the progress of bioinspired materials based on silk. We first give a brief introduction of silk, covering its sources, features, extraction, and forms. Then, we summarize the preparation and application of silk-based materials mimicking bone, nacre, skin, and polar bear hair. Finally, we discuss the current challenges and future prospects of the development of silk-based bioinspired materials. This review

[1]Institute of Applied Bioresources, College of Animal Sciences, Zhejiang University, Hangzhou 310058, China

[2]Key Laboratory of Utilization and Innovation of Silkworm and Bee Resources of Zhejiang Province, Zhejiang University, Hangzhou 310058, China

[3]MOE Key Laboratory of Macromolecular Synthesis and Functionalization, Department of Polymer Science and Engineering, Key Laboratory of Adsorption and Separation Materials & Technologies of Zhejiang Province, Zhejiang University, Hangzhou 310027, China

[4]State Key Laboratory of Chemical Engineering, College of Chemical and Biological Engineering, Zhejiang University, Hangzhou 310027, China

*Correspondence: wwgao@zju.edu.cn (W.G.), hbai@zju.edu.cn (H.B.)

https://doi.org/10.1016/j.isci.2022.103940

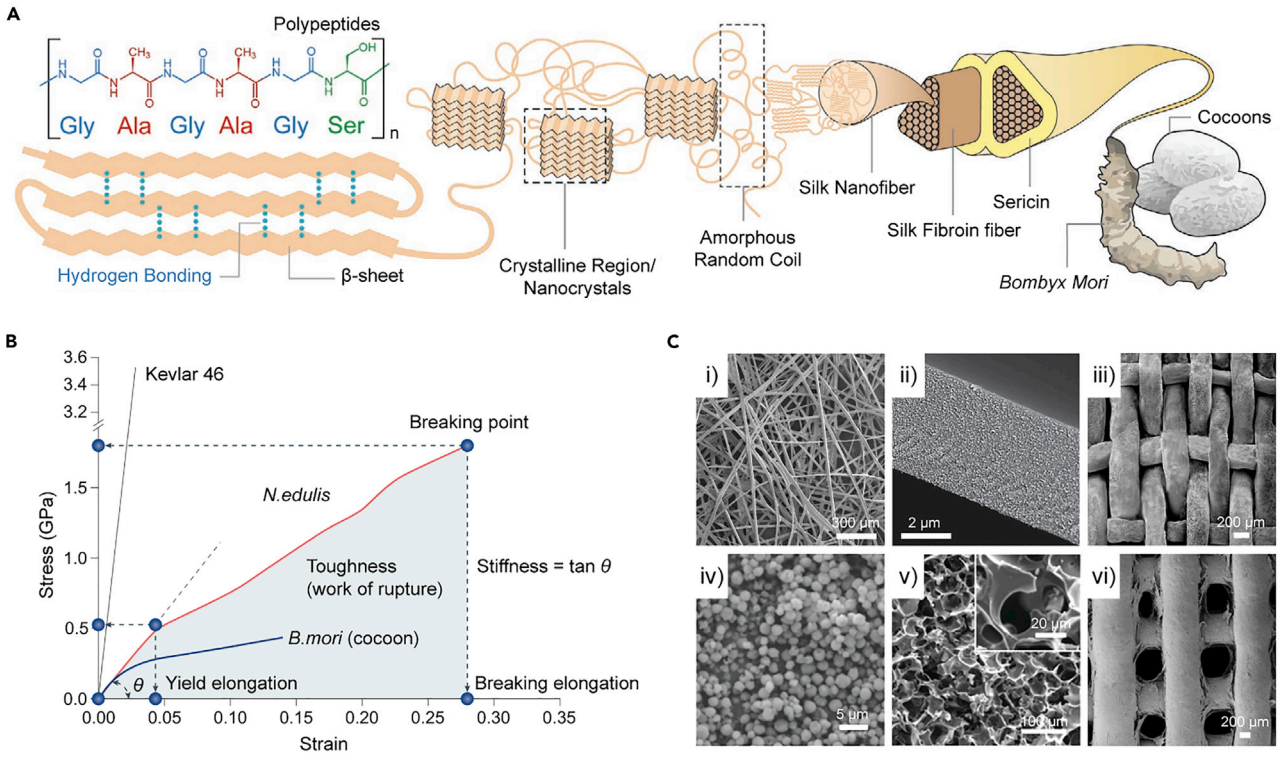

Figure 1. A brief overview of silk including its hierarchical structures, mechanical performance, and assembled materials

(A) Illustration of the hierarchical structures of silk fiber from *B. mori*. Adapted with permission from Li et al. (2021). Copyright 2021, Wiley-VCH.

(B) Stress–strain curves of a dragline silk fiber produced by the spider *Nephila edulis* (*N. edulis*), a silk fiber produced by the silkworm *B. mori* and a para-aramid synthetic fiber Kevlar 46. Adapted with permission from Ling et al. (2018b). Copyright 2018, Springer Nature.

(C) A series of silk-based materials in applications: i) SEM image of a silk fiber mat produced by silkworm spinning on a plate. Adapted with permission from Xu et al. (2020). Copyright 2020, Wiley-VCH. ii) Cross-sectional SEM image of a silk membrane prepared from liquid exfoliated SNF. Adapted with permission from Ling et al. (2016b). Copyright 2016, Wiley-VCH. iii) SEM image of a woven textile of biomimetic porous silk fibers. Adapted with permission from Cui et al. (2018). Copyright 2018, Wiley-VCH. iv) SEM image of silk microspheres and v) SEM image of a silk porous scaffold. Adapted with permission from Wang et al. (2017). Copyright 2017, the Royal Society of Chemistry. vi) SEM image of a 3D-printed silk construct. Adapted with permission from Fitzpatrick et al. (2021). Copyright 2021, Elsevier.

provides a better understanding to silk's roles in biomimetic composites, which will further inspire scientists and engineers to explore its potential applications.

SILK

Sources

Silk can be produced by spiders, silkworms, and other arthropods, with the basic component being proteins. Owing to the difficulties in raising spiders and collecting their silk, spider silk is not extensively applied on a large scale. In contrast, cocoon silk derived from silkworms, especially the species of *Bombyx mori* (*B. mori*), have been used worldwide for thousands of years, making it the most abundant source of silk protein. Some wild silkworms, like *Antheraea pernyi* (*A. pernyi*) and *Antheraea mylitta* (*A. mylitta*), can also yield high-quality silk (Chen et al., 2012; Fu et al., 2011, 2019). Additionally, recent developments of transgenic technology make it possible to produce recombinant spider silk protein via diverse expression systems, such as *E.coli*, yeast, plants, goat, as well as silkworms (Aigner et al., 2018; Long et al., 2021; Scheller et al., 2001; Teule et al., 2012; Whittall et al., 2021), thus further expanding silk's sources and meanwhile achieving the customization of fusion silk proteins.

Features

Silk is known for unrivalled mechanical properties, originating from the hierarchical structures from molecular to macroscopic scale (Figure 1A). The amino acid sequences aggregate into specific domains with nanosized β-crystalline phase imbedding in an amorphous matrix, where the crystalline domain determines

strength and the amorphous domain decides toughness (Ling et al., 2018b; Omenetto and Kaplan, 2010; Wegst et al., 2015). The aggregation structures further assemble into highly oriented nanofibers, then to microfibers and macro-fibers, forming massive inter- and intramolecular hydrogen bonds at multiscale, which endows silk fiber with both high strength and toughness (Figure 1B). For example, spider silk shows a stiffness of 10–12 GPa, ultimate tensile strength of 0.9–1.4 GPa, and breaking elongation of 30%–60%; toughness in particular, reaches up to 160–240 MJ/m^3, greatly exceeding steel, carbon fiber, glass fiber, and Kevlar fiber (Omenetto and Kaplan, 2010; Yarger et al., 2018). Regarding to *B. mori* silk, its stiffness, ultimate tensile strength, breaking elongation, and toughness are 5–10 GPa, 300–600 MPa, 10%–25%, and ~70 MJ/m^3, respectively, which are also superior to many synthetic fibers (Shah et al., 2014; Yang et al., 2019b). The excellent mechanical properties endow macroscale silk fibers with a broad range of uses during the long history, such as textile, suture, parachute, and even body armor. In addition, silk microfibers (SMF) and silk nanofibers (SNF), the mesoscale building blocks of silk fiber, also show great potential for electronic and environmental applications. When directly exfoliated from silk fibers, SMF and SNF are able to retain their intrinsic features and can be further processed into high-performance materials, which are expected to be used as filtration systems, biosensors, electrical, and optical devices.

Moreover, due to good biocompatibility and controllable biodegradability, cocoon silk has been approved by U.S. Food and Drug Administration (Bhattacharjee et al., 2017; Farokhi et al., 2018). Many *in vitro* and *in vivo* studies have confirmed that silk protein shows very low immunogenicity, and is able to promote cell growth and tissue regeneration (Kundu et al., 2013; Wenk et al., 2011), indicating its great potential in biomedical engineering.

Extraction

Silk fibers can be reeled from silkworm cocoons by factory equipment in large scale, which are mainly applied in textile industry. Meanwhile, regenerated silk fibroin (RSF) is playing a dominated role in building silk-based materials of diverse forms. Currently, a standard procedure for RSF extraction from *B. mori* cocoons has been established (Rockwood et al., 2011), which typically includes degumming, rinsing, dissolution, dialysis, and centrifugation. Generally, inorganic salts such as high concentration of LiBr solution, NaSCN solution, $ZnCl_2$ solution, and a ternary solvent of $CaCl_2$/ethanol/H_2O are used to dissolve degummed silk fibers by breaking hydrogen bonds and disassembling the β-crystalline structures, and after completely removing the ions and impurities, an aqueous solution of pure RSF is obtained. The RSF solution can be lyophilized for long-term storage, and the lyophilized stuff is able to be dissolved in organic solvent like HFIP (1,1,1,3,3,3-hexafluoro-2-propanol) to prepare other forms of materials. Some organic salts like AminCl and BminCl can dissolve silk fibers as well, to obtain relatively high concentration of RSF ionic liquid solution, and they are recyclable. In addition, as silk contains a considerable percentage of amino acids with side chains, such as serine, threonine, aspartic, glutamic, and tyrosine, the RSF molecules expose abundant reactive sites for further chemical and functional modification (Murphy and Kaplan, 2009). But it should be noted that the degumming treatment and dissolution process inevitably impair the mechanical properties of post-prepared RSF materials, due to the breakage of silk fibroin peptide chains and macromolecular degradation (Ho et al., 2012; Jin et al., 2015; Yang et al., 2020). On one hand, using non-alkali solution (like urea) rather than alkali solution (like sodium carbonate) for degumming will decrease the damage to silk fibers (Yang et al., 2020). On the other hand, because the dissolved RSF molecules present as random coils, it is feasible to regulate the mechanical features of RSF materials by tuning their conformational transition to β-crystalline structures, which will meet the demands in various application scenarios (Guo et al., 2020; Hu et al., 2011).

Besides RSF molecules, SNF also play an important role as building blocks to construct bioinspired materials. Top-down exfoliation, bottom-up assembly, and electrospinning have been verified as effective methods for the preparation of SNF, which show specific advantages as well as disadvantages. The exfoliation method usually contains three steps: firstly, silk fibers are immersed in HFIP and incubated at 60°C for 24 h to obtain silk fiber/SMF slurries; then, the dried silk fiber slurries is transferred to H_2O solution and precipitates are removed; finally, SMF dispersion is treated by ultrasound to extract SNF (Ling et al., 2016b). Although multiple steps are required in this process, the exfoliated SNF retain their natural structure and physical properties. For the bottom-up method, low concentration of aqueous RSF solution is heated at 60°C for one week to assemble silk proteins into SNF (Ling et al., 2018a). Driven thermodynamically, this process often requires appropriate conditions and fairly long time, but once started SNF will grow spontaneously and no further energy is needed. Electrospinning indicates a technique to allow charged silk

solution extruding through a needle and spraying as nanofibers, which then deposited on an oppositely charged collector (Humenik et al., 2018). Because of the precise control of processing conditions, SNF's morphologies and arrangements can be well tuned. However, post-treatments are usually required to improve the mechanical property and water stability of the as-prepared SNF.

Forms

Silk shows favorable versatility (Figure 1C) not just limited to some fiber forms, including single fiber, yarns, and fabrics, as well as short fibers obtained via chopping or milling (Li et al., 2015; Ude et al., 2014; Xu et al., 2015). More interestingly, RSF can be processed into a series of non-fibrous forms (Koh et al., 2015; Omenetto and Kaplan, 2010; Rockwood et al., 2011), such as films, scaffolds, hydrogels, microspheres, and nonwovens, which will meet the requirements for building different types of bioinspired materials. For example, a silk scaffold shows similar porous structures to spongy bone, with the ability to support the adhesion and proliferation of mesenchymal stem cells (MSCs) (Bhattacharjee et al., 2017). Besides the above, several novel forms of silk have been developed recently. By changing the spinning behavior of *B. mori* silkworms, we reported a flat silk cocoon significantly different from the common silk cocoon both in shape and size, which was used as reinforcing fiber networks in a skin-inspired composite film (Xu et al., 2020). Another example also came from a fiber-reinforced composite, where a hybrid woven fabric consisting of silk fibers from *A. pernyi* silkworms and carbon fibers significantly improved the impact resistance of the resin matrix (Yang et al., 2019b).

BONE-INSPIRED MATERIALS BASED ON SILK

Bone presents as a very typical biological composite material with sophisticated hierarchies (Figure 2A) (Reznikov et al., 2018; Wegst et al., 2015). With hydroxyapatite (HAP) nanocrystals distributing along the collagen fibrils made from type-I collagen molecules, the organic–inorganic phases are tightly integrated at nanoscale and further assembly into macroscale structures. As a vitally important support for human body, bone perfectly combines high strength and toughness, which are usually considered to be mutually exclusive. Bone also has the ability of self-growing and self-healing, ensuring its normal health and function. Inspired by the chemical composition, multiscale architecture, and multifunction of bone, many bone-like composites have been constructed, most of which are applied for bone tissue engineering. In this respect, silk serves as a fascinating material due to numerous advantages (Bhattacharjee et al., 2017; Melke et al., 2016; Saleem et al., 2020), such as its similar fibrous protein structure to type-I collagen, favorable biomineralization ability, outstanding mechanical properties, and low immunogenicity. As the impressive performance of silk/HAP composites in bone tissue engineering have been extensively reported, here we will provide introductions to several studies with great significance.

In 2009, Collins et al. presented the first example of a biomimetic bone-like silk/HAP composite scaffold that was load bearing with mechanical properties comparable to cancellous bone (Collins et al., 2009). In comparison with the compressive strengths of collagen scaffolds (~0.034 MPa) and commercial calcium phosphate scaffolds (< 5 MPa), such macroporous scaffold exhibited average strength of 14 MPa and modulus of 175 MPa, which were even in the middle range for cancellous bone's mechanics (7–10 MPa and 5–500 MPa, respectively). The scaffold was prepared by slowly infiltrating a frozen phosphate-containing silk fibroin gel with Ca^{2+} ions and the following ethanol treatment and chemical cross-linking, achieving uniform *in situ* mineralization and tight protein/mineral integration. Moreover, the silk/HAP scaffold could promote the proliferation of human bone marrow stromal cells (HBMSCs) *in vitro*, and new osteoid was observed on the surface of the scaffold when subcutaneously implanted in mice, suggesting its potential to be used as an implantable alternative to allograft, autograft, and xenograft. This study opened a new way to build silk/HAP composite scaffolds instead of directly mixing the two components, which usually resulted in phase separation and poor mechanics.

Recently, Farokhi et al. systematically summarized silk/HAP composites for bone tissue engineering in a review article (Figure 3) (Farokhi et al., 2018), where they could be applied alone or in combination with bioactive molecules and stem cells to further improve the repair outcomes. For example, a silk-nanohydroxyapatite (nHAP) scaffold loading with bone morphogenetic protein-2 (BMP-2) and vascular endothelial growth factor (VEGF) was developed for bone regeneration (Figure 4A), as BMP-2 was confirmed to induce osteogenic differentiation and VEGF played an important role in blood vessel formation (Wang et al., 2017). The controlled dual release of BMP-2 and VEGF synergistically promoted osteogenesis both *in vitro* and *in vivo*; according to newly formed bone content at 12 weeks post implantation in rat calvarial

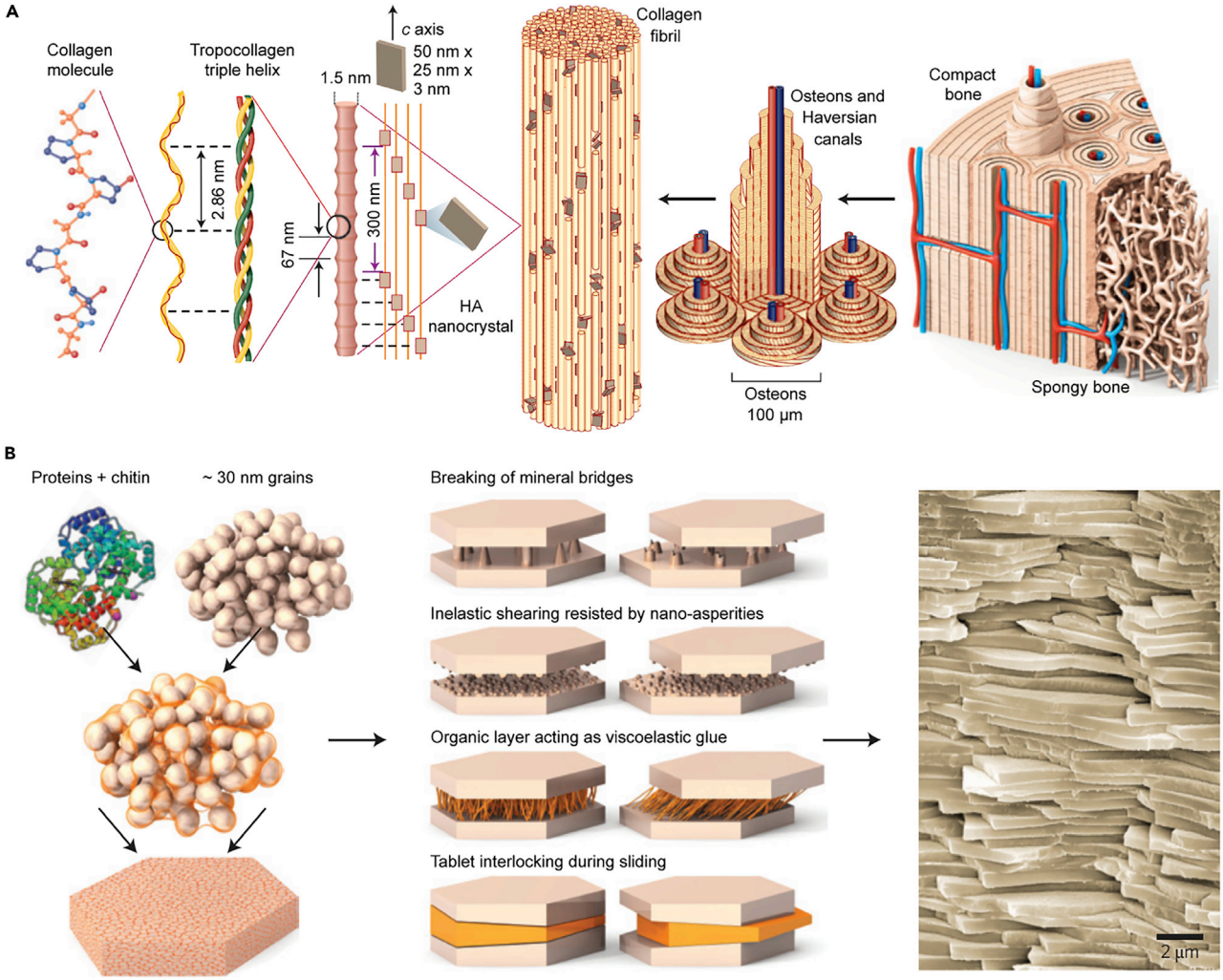

Figure 2. Hierarchical structures of bone and nacre

(A) Osteons have a lamellar structure, with individual lamella consisting of fibers arranged in geometrical patterns. The fibers comprise several mineralized collagen fibrils, composed of collagen protein molecules (tropocollagen) formed from three chains of amino acids and nanocrystals of hydroxyapatite, and linked by an organic phase to form fibril arrays.

(B) Nacre is a brick-and-mortar structure of $CaCO_3$ mineral platelets (aragonite), which provide strength and proteins, which allow for ductility and toughness. Adapted with permission from Wegst et al. (2015). Copyright 2014, Springer Nature.

defects, the composite scaffold achieved the best bone formation effect compared with adding BMP-2 or VEGF alone. Additionally, VEGF could facilitate the vascularization and accelerate the degradation of the silk scaffold, which also led to enhanced bone regeneration. Apart from similarities in both composition and structure to natural bone, a perfect match between the implant and the patient's anatomy is required. In this regard, 3D printing is emerging as a more promising technique, due to its customized design and precise control in constructing bone tissue engineering scaffolds. In 2021, Fitzpatrick et al. reported a 3D-printed silk/HAP scaffolds with controlled microporosity and interconnected pores throughout (Figure 4B) (Fitzpatrick et al., 2021). This construct exhibited not only mechanical properties suitable for bone but also good cytocompatibility and osteoconductivity. Indeed, 3D printing provides a possible path to truly replicate bone's fine architectures at multiscale in the future.

NACRE-INSPIRED MATERIALS BASED ON SILK

As with bone, nacre is also a laminated composite, where the layered aragonite ($CaCO_3$) platelets are bonded by a thin layer of organic component (Du et al., 2019b; Gerhard et al., 2017). Nacre achieves desirable integration of inorganic–organic phases with stable and strong interfacial interactions (Figure 2B),

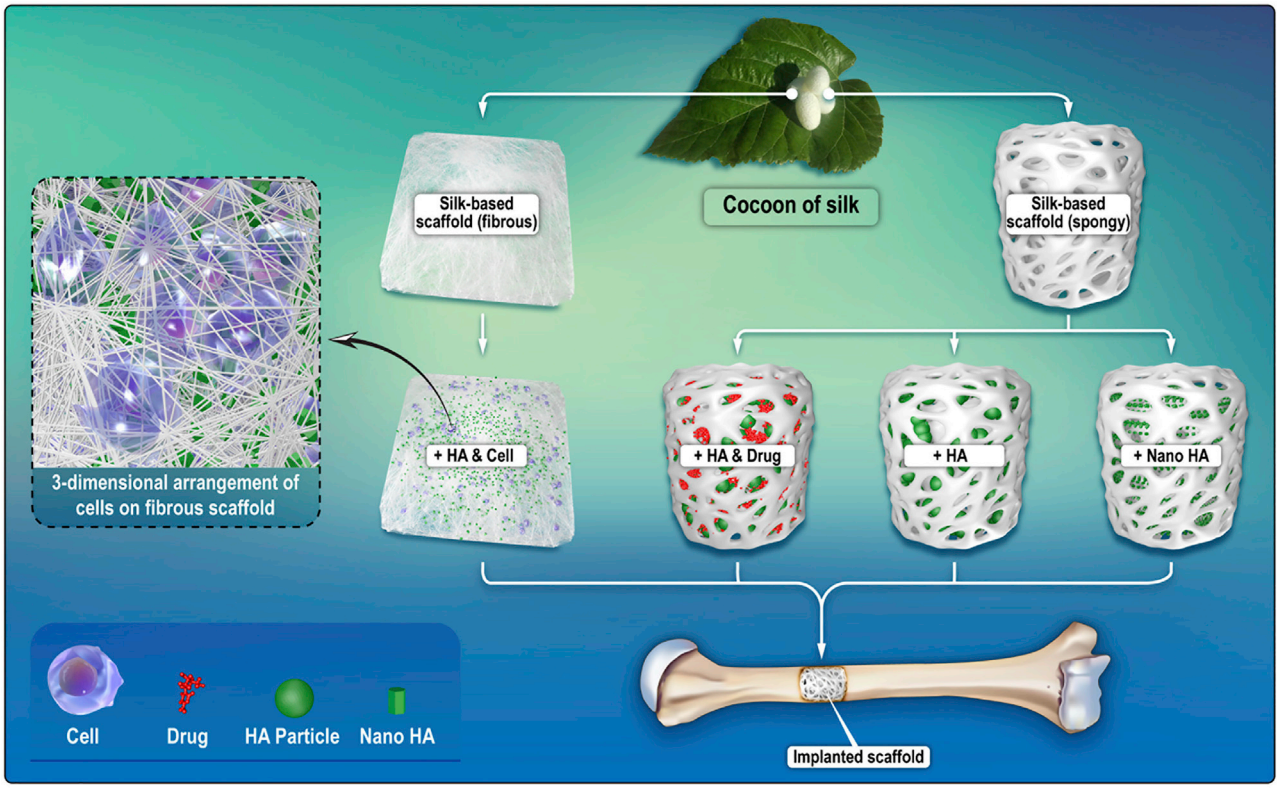

Figure 3. Schematic of different types of silk/hydroxyapatite composites for bone tissue engineering
Adapted with permission from Farokhi et al. (2018). Copyright 2017, Elsevier.

which endows it with remarkable mechanical properties combining both high strength and toughness (Barthelat et al., 2016; Gao et al., 2020; Wegst et al., 2015). In order to build lamellar structures, numerous approaches have been proposed including vacuum filtration, spin-assisted layer-by-layer assembly, solution casting, hot-press-assisted slip casting, and vacuum filtration tend to be the most frequently used method for silk-based nacre-like composites. Owing to favorable mechanical properties and abundant surface charges, SNF directly exfoliated from silk fibers or self-assembled from RSF molecules have been widely used as building blocks to construct nanofluidic channel systems, which exhibit low resistance and high efficiency in ion selection, osmotic energy harvesting, water treatment, and so on (Chen et al., 2020; Ling et al., 2016a, 2017a; Xin et al., 2019, 2020, 2021).

For instance, Xin et al. constructed a multilayer graphene oxide-SNF-graphene oxide (GO-SNF-GO) biomimetic sandwich via vacuum filtration (Figure 5) (Xin et al., 2020). In these nacre-like structures, SNF were considered to serve as "nanoscale locks" to crosslink the GO sheets, resulting from a strong combination of hydrogen bonds and nonbonded interactions. Besides the distinct amphiphilic features of SNF surface for enhancing the interlayer interactions, SNF retained the structural hierarchy and well-organized β-sheet structures of natural silk, which greatly contributed to mechanical performance of the composites. As a result, compared with GO membrane, the tensile strength of GO/SNF/GO membrane increased from 52 to 364.2 MPa, and the toughness increased from 1.01 to 12.51 MJ/m^3, both with the optimal SNF content of 78.7 wt%. When used as an osmotic power generator, the GO/SNF/GO membranes exhibited long-term stability in saline. More importantly, with the SNF significantly increasing the surface charge densities to promote ion transport, the composite membrane achieved excellent osmotic energy conversion.

Similarly, Ling et al. constructed a SNF/HAP membrane by vacuum filtration, showing highly ordered multilayer structures with alternated HAP and SNF layers (Figure 6) (Ling et al., 2017a). During processing, the SNF served as *in situ* templates for mineral formation, and the grown HAP nanocrystals were stabilized by the connected SNF networks. Owing to the protein/mineral combination and nacre-like structure, the SNF/HAP membrane exhibited excellent mechanical properties. A 37-μm-thick membrane had a modulus

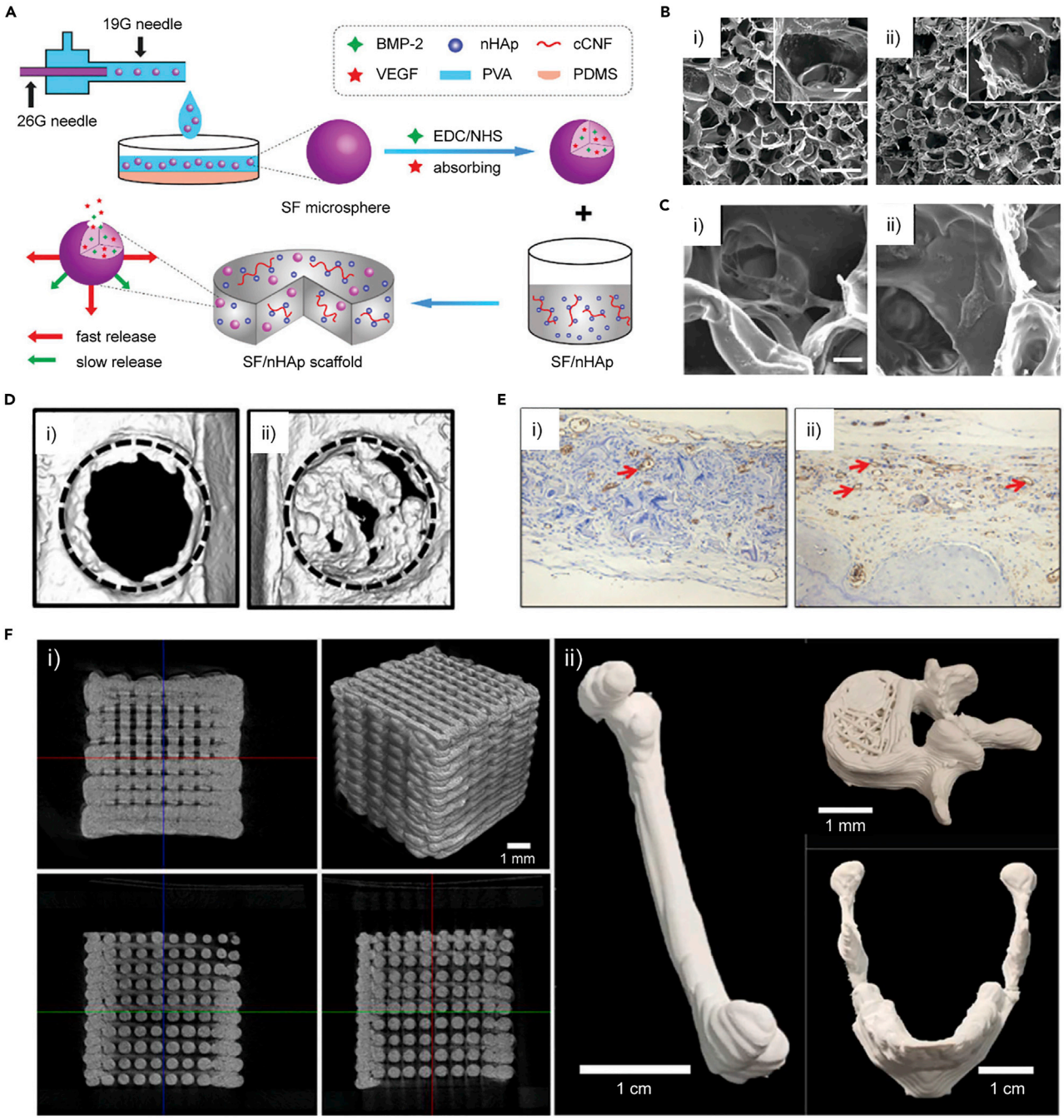

Figure 4. Two types of silk/hydroxyapatite scaffolds for bone tissue engineering

(A) Schematic of the preparation of the silk fibroin/nHAP scaffold loading with dual growth factors of BMP-2 and VEGF (B + V scaffold).

(B) SEM images of i) control scaffold (without growth factor) and ii) B + V scaffold, scale bars are 100 and 20 μm.

(C) SEM images of cell adhesion on i) control scaffold and ii) B + V scaffold, scale bar is 10 μm.

(D) μCT images of the newly formed bone at 12 weeks post implantation with i) control scaffold and ii) B + V scaffold.

(E) Blood vessel analysis of the specimen of critical-sized calvarial defects at 12 weeks post implantation with i) control scaffold and ii) B + V scaffold. The red arrows show the typical brown, round or oval structures, which indicate the presence of blood vessels. A–E, adapted with permission from Wang et al. (2017). Copyright 2017, the Royal Society of Chemistry.

(F) i) Microcomputed tomography of a 3D-printed cube showing the general aspect of the cube (top right), regular filament distribution, and interconnected pores; ii) 3D-printed anatomical structures: femur (left), vertebra (right, top), and mandible (right, bottom). Adapted with permission from Fitzpatrick et al. (2021). Copyright 2021, Elsevier.

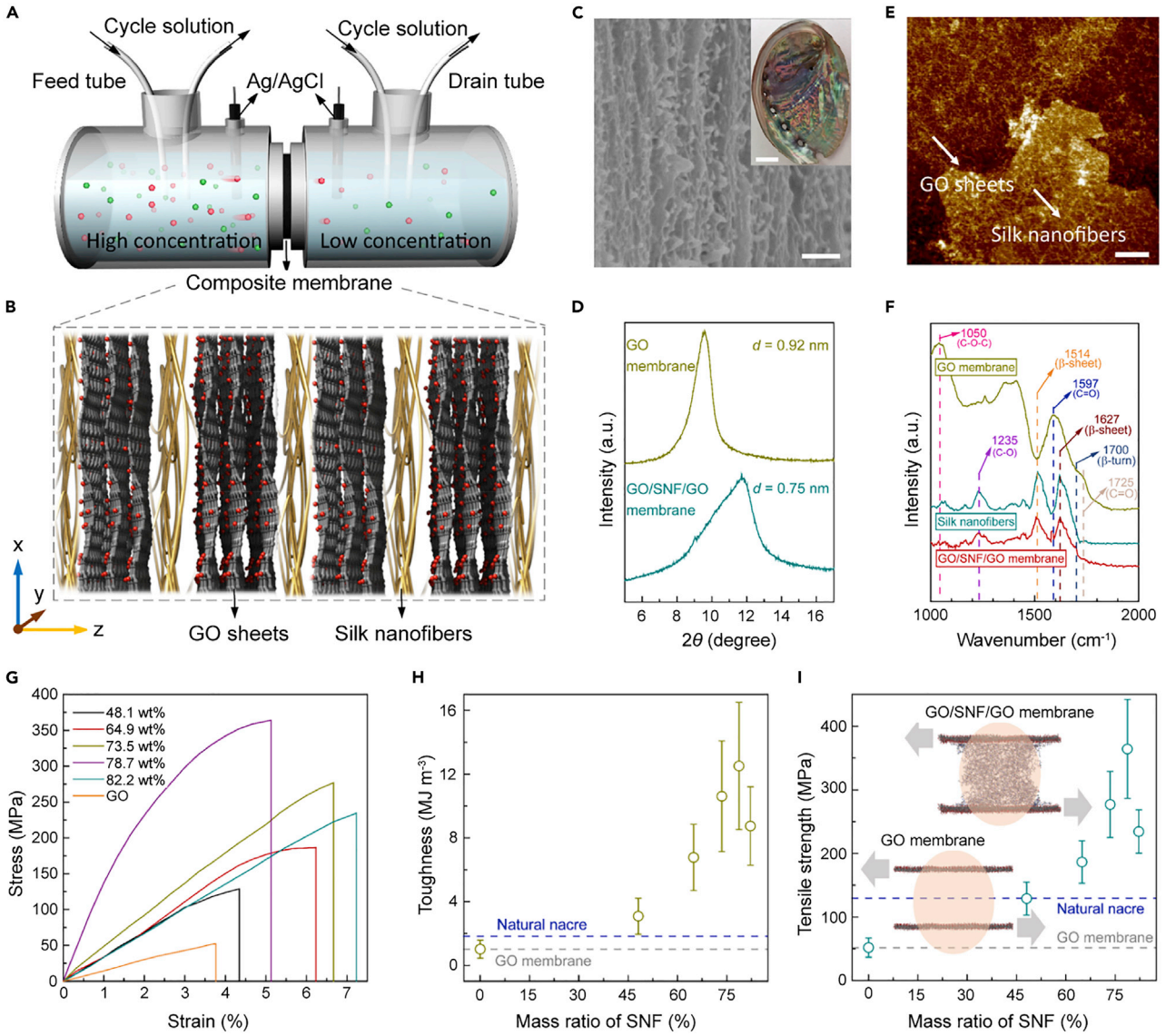

Figure 5. The structure and mechanical properties of the GO/SNF/GO membrane as a nanofluidic device to harvest osmotic energy

(A) Schematic of the experimental setup for monitoring fluid transmembrane transport.

(B) The multilayer assembly of the GO/SNF/GO membrane.

(C) SEM image evidencing the sandwich-like architecture of the composite membrane mimicking nacre, scale bar is 200 nm.

(D) XRD measurements for estimating the change in interlayer spacing *d*.

(E) GO/SNF/GO composite structures constructed by amphiphilicity-driven assembly, scale bar is 500 nm.

(F) FTIR spectra acquired from the GO membrane, SNFs, and GO/SNF/GO membrane.

(G) Stress–strain curves of GO and GO/SNF/GO membranes with different SNF contents.

(H) Toughness-mass ratio of SNF curves of different membranes.

(I) Tensile strength-mass ratio of SNF curves. Adapted with permission from Xin et al. (2020). Copyright 2020, American Chemical Society.

of 7.7 ± 0.2 GPa, around three times higher than that of pristine self-assembled SNF membrane (2.25 ± 0.25 GPa), and a toughness of 1.7 ± 0.3 MJ/m^3, 10 to 100 times higher than that of SNF membranes (0.09–0.2 MJ/m^3). Such low-cost and rapid-formation multilayer SNF/HAP membranes with good durability could be universally and efficiently used in water purification for dyes, proteins, nanocolloids, and in particular, heavy metal ions. In another study from the same group, chitin nanofibrils (CNF) as the third component was further introduced to the SNF/HAP system (Ling et al., 2018a). As confirmed to be critical for mechanical toughening in natural nacre, CNF also induced sufficient interfibrillar sliding as well as fibrils' pulling in

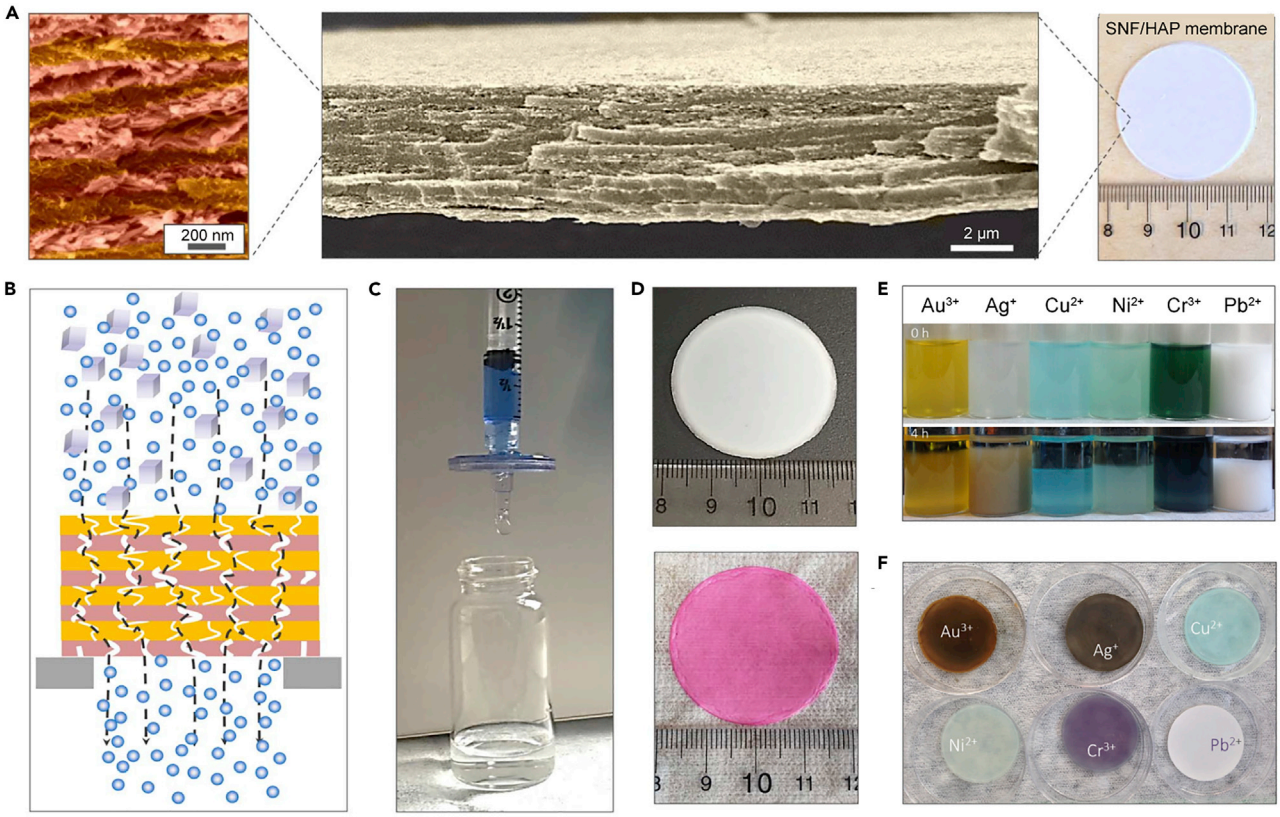

Figure 6. Structure and separation performance of SNF/HAP membranes

(A) SEM images showing the nacre-like, highly ordered multilayer structures of a SNF/HAP membrane.

(B) Cross-sectional representation of a multilayer SNF/HAP membrane to filter compounds.

(C) A photograph showing the successful rejection of Alcian Blue 8GX by the SNF/HAP-based syringe nanofilter.

(D) SNF/HAP nanofiltration membrane before and after filtration with Rhodamine B solution.

(E) Photographs of SNF/HAP dispersion-adsorbed metal ions at 0 and 24 h.

(F) Photograph of an SNF/HAP membrane after metal ions were adsorbed through flux-controllable filtration. Adapted under the terms and conditions of CC BY license. Ling et al. (2017a). Copyright 2017, The Authors. Published by American Association for the Advancement of Science.

the current ternary composite, thus synergistically increasing its strength and toughness. Despite many other silk-based nacre-like nanocomposites having been developed in recent years, they are generally limited to thin films with thickness in several to dozens of micrometers (Bandar Abadi et al., 2021; Li et al., 2020b; Wang et al., 2016), which may not be suitable for use as bulk structural materials.

SKIN-INSPIRED MATERIALS BASED ON SILK

Skin not only provides vertebrates with a protection barrier from the outer environment but also features as a comprehensive sensor capable of responding to multiple external stimuli simultaneously (Liu et al., 2019a; Ni Annaidh et al., 2012). Skin is also soft, tough, stretchable, and self-healable, which has attracted tremendous attention to mimic its structure and function in flexible electronics, smart materials, and wound healing. Particularly, the past decades have witnessed the rapid development of skin-inspired flexible electronics (Chortos and Bao, 2014; Wang et al., 2021a; Yu et al., 2018). In this context, the mechanical robustness, structural flexibility, demic affinity, and environmental sustainability of silk make it a promising base material in this thriving field. As several recent review articles have described in detail the applications of silk-based materials for different flexible electronics including conductors, sensors, actuators, and optical devices (Shi et al., 2021; Wang et al., 2019a; Zhu et al., 2016), herein, we will mainly focus on the biomimetic structure design inspired by skin.

Skin consists of three layers with epidermis, dermis, and endodermis, where the dermis as the thickest layer plays a dominated role for bearing deformation and preventing damage (Figure 7A) (Yang et al., 2015). Inspired from the 3D network structures constructed by tough and elastic fibers in the dermis, Wang et al. reported a

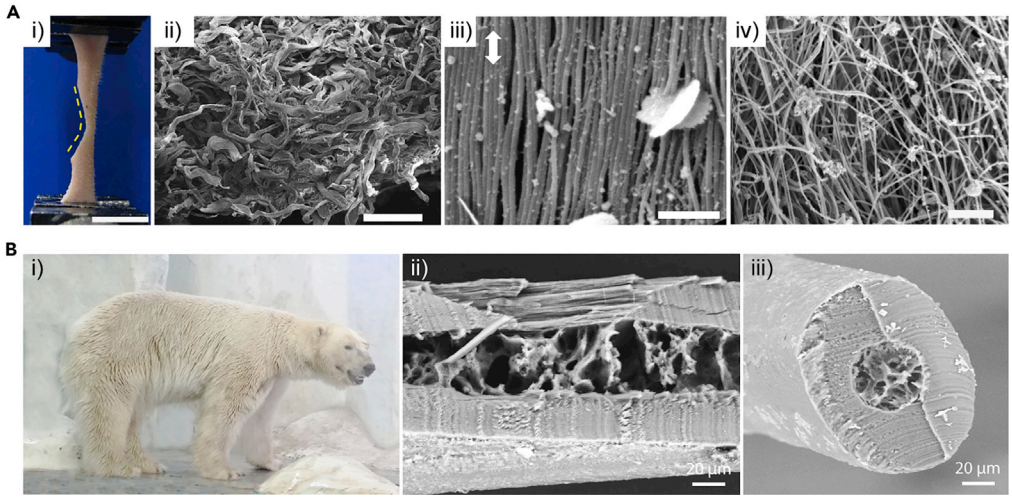

Figure 7. Morphology and microstructure of prenotched rabbit skin and polar bear hairs

(A) i) Photograph of prenotched rabbit skin under uniaxial tensile loading, scale bar is 10 mm; ii) SEM image showing the disordered arrangement of curved collagen fibers in skin, scale bar is 50 μm; iii)collagen fibrils at notched side are delaminated, aligning close to the tension direction after loading (with arrow indicating the loading direction), scale bar is 1 μm; iv) collagen fibrils at unnotched side are delaminated/relaxed after loading/unloading, scale bar is 2 μm. Adapted under the terms and conditions of CC BY license. Yang et al. (2015). Copyright 2015, The Authors. Published by Springer Nature.

(B) i) Photograph of a polar bear; ii, iii) SEM images showing the hollow core and aligned shell of a polar bear hair, respectively. Adapted with permission from Cui et al. (2018). Copyright 2018, Wiley-VCH.

biomimetic gel sensor based on silk fibroin/cellulose nanocrystals (CNC) as a "tough" unit and polyacrylamide (PAM) as an "elastic" segment, named SCP gel (Figure 8) (Wang et al., 2021b). The addition of CNC promoted the conformation transition of silk fibroin from α-helixes into β-crystallites, which in combination with silk fibrous networks and multiple hydrogen bonding in SCP gel effectively increased the mechanical stability of the integrated structure. The SCP gel was able to maintain 88.8% of maximum strength under a deformation of 40% after 1000 compression cycles. The SCP gel also exhibited considerable adhesion property and self-healing capability, which would be favorable for their application as sensors attached directly to human skin (Wang et al., 2019b). In this study, the SCP gel's applications were well demonstrated, either as a sensor to detect large/subtle human motions and toxic gas atmosphere, or as a visual temperature indicator, suggesting its multifunctional potential in flexible electronics.

Besides high strength and toughness, skin shows dramatic tear resistance, originating from the rearrangement of collagen fibers in dermis when stretched (Figure 7A) (Yang et al., 2015). This feature is also quite essential for flexible electronics, because defects are usually inevitable during their processing and utilization, especially for those with pure polymer supporting substrates. Take the most commonly used polymer PDMS as an example, both its tensile strength and fracture strain would decrease by 90% when a notch existed. To address this need, we replicated skin's stress redistribution strategy in a fiber-reinforced composite film based on flat silk cocoon, and achieved significant mechanical efficiency and outstanding tear resistance (Figure 9) (Xu et al., 2020). Compared with pure polymer, integrating only 1 wt% of silk fiber could lead to a 300% and 612% improvement in tensile strength and modulus, while the composite film still maintained fiexibility and transparency. In addition, the composite film displayed remarkable tear and fatigue resistance withstanding nearly 30,000 loading–unloading tensile cycles, about 7.5 times that of the pure film. The excellent mechanical performance was achieved by the synergistic effect of fiat silk cocoon serving as both reinforcing phase and crack inhibitor in the polymer matrix. More interestingly, this study proposed the production of a novel form of silk fibers with unique function by simply changing silkworms' spinning behaviors, which would stimulate the development of silk-fiber-reinforced composite materials.

POLAR-BEAR-HAIR-INSPIRED MATERIALS BASED ON SILK

Polar bear hairs present hollow structures with randomly porous core and aligned shell (Figure 7B) (Cui et al., 2018; Shao et al., 2020; Wang et al., 2020a; Zhao et al., 2014), which play a vital role in keeping

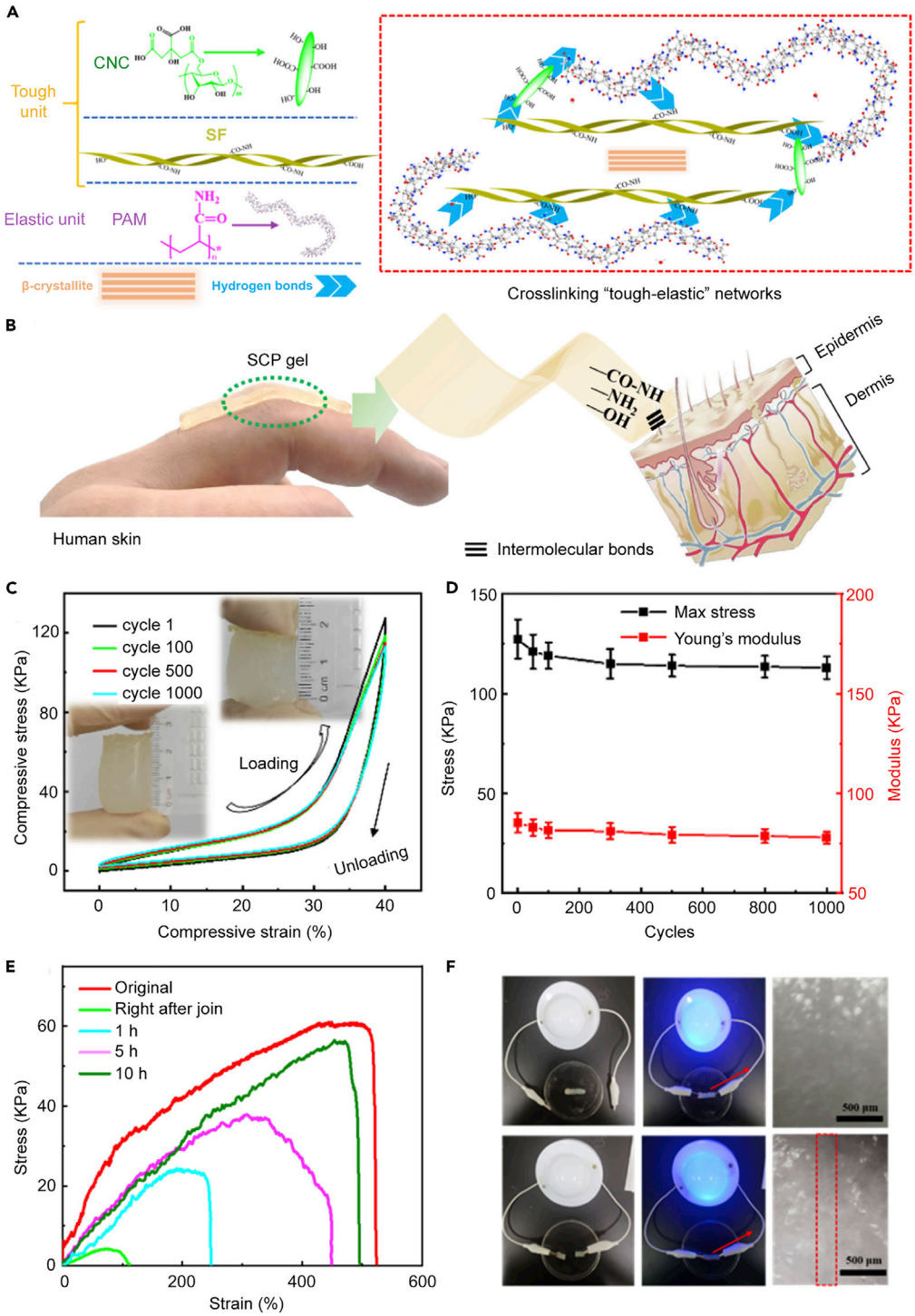

Figure 8. A multifunctional gel made with silk fibroin imitating skin

(A) The cross-linking networks formed by hydrogen bonds in SCP gel.

(B) A photo and schematic illustration of SCP gel adhered to skin through intermolecular bonds.

(C and D) Repeated compression test with 40% of strain showing the good stability of SCP gel.

(E) Stress–strain curves of SCP gel and gels healed for different times.

(F) The relighted LED showing the instantaneous healing of the cut gel strip when joined. Adapted with permission from Wang et al. (2021b). Copyright 2021, American Chemical Society.

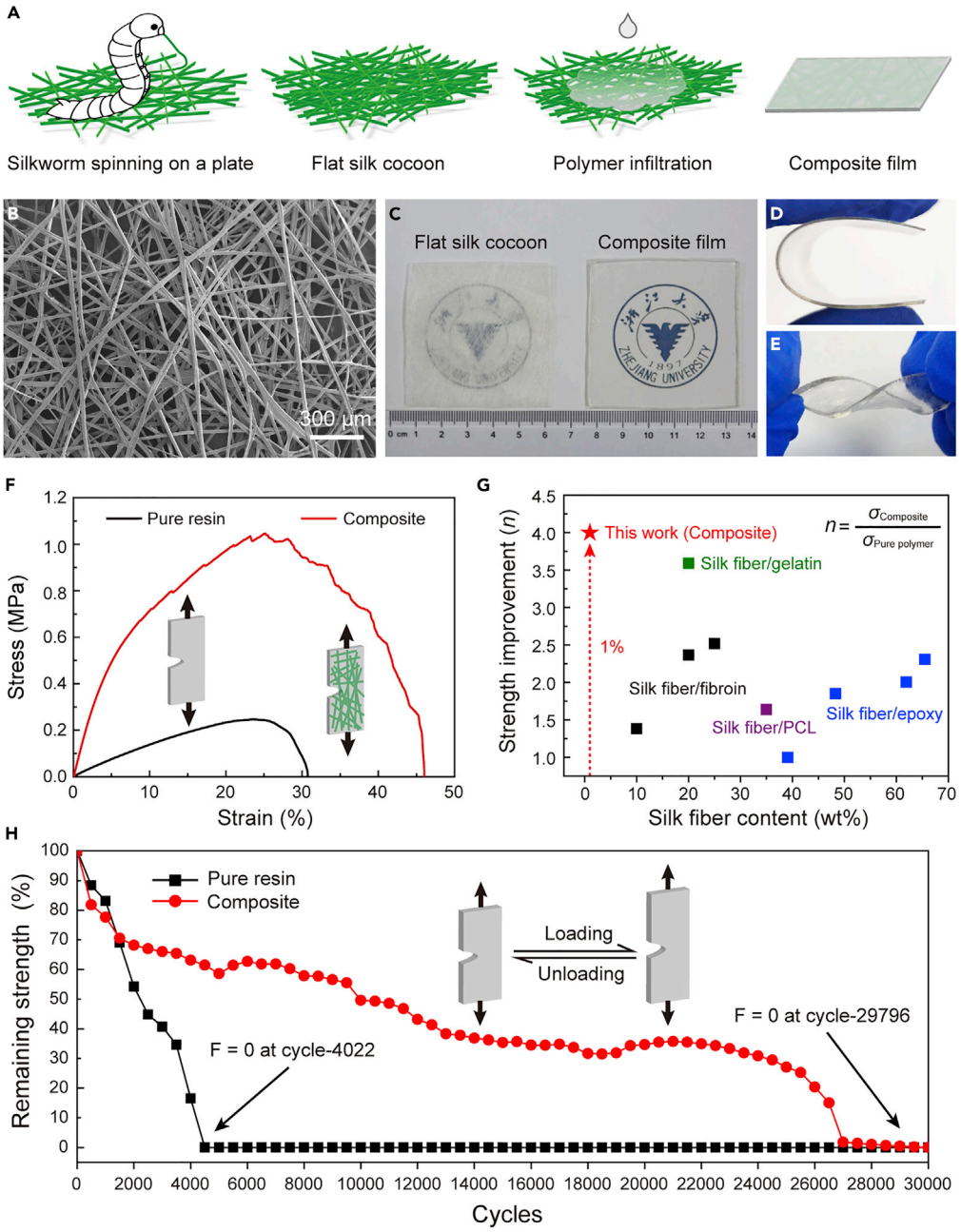

Figure 9. The fabrication, morphology, and mechanical properties of a skin-inspired composite film

(A) Schematic illustration of the fabrication process of the composite film based on fiat silk cocoons.

(B) SEM image showing the randomly fibrous structure of a fiat silk cocoon.

(C) Optical photograph of the fiat silk cocoon and as-prepared transparent composite film.

(D and E) Bending and twisting of the transparent composite film.

(F) Stress–strain curves of prenotched pure resin and composite films under monotonic loading.

(G) Comparative results showing the most significant mechanical reinforcing effect of this study.

(H) Loading–unloading tests showing the outstanding tear and fatigue resistance of composite film. Adapted with permission from Xu et al. (2020). Copyright 2020, Wiley-VCH.

warm in the extremely cold environment for polar bears. Mimicking such structural design in synthetic fibers will contribute to the fabrication of thermally insulating textiles, but it still remains a challenge to achieve continuous and large-scale production. To this end, Cui et al. reported a "freeze-spinning" technique

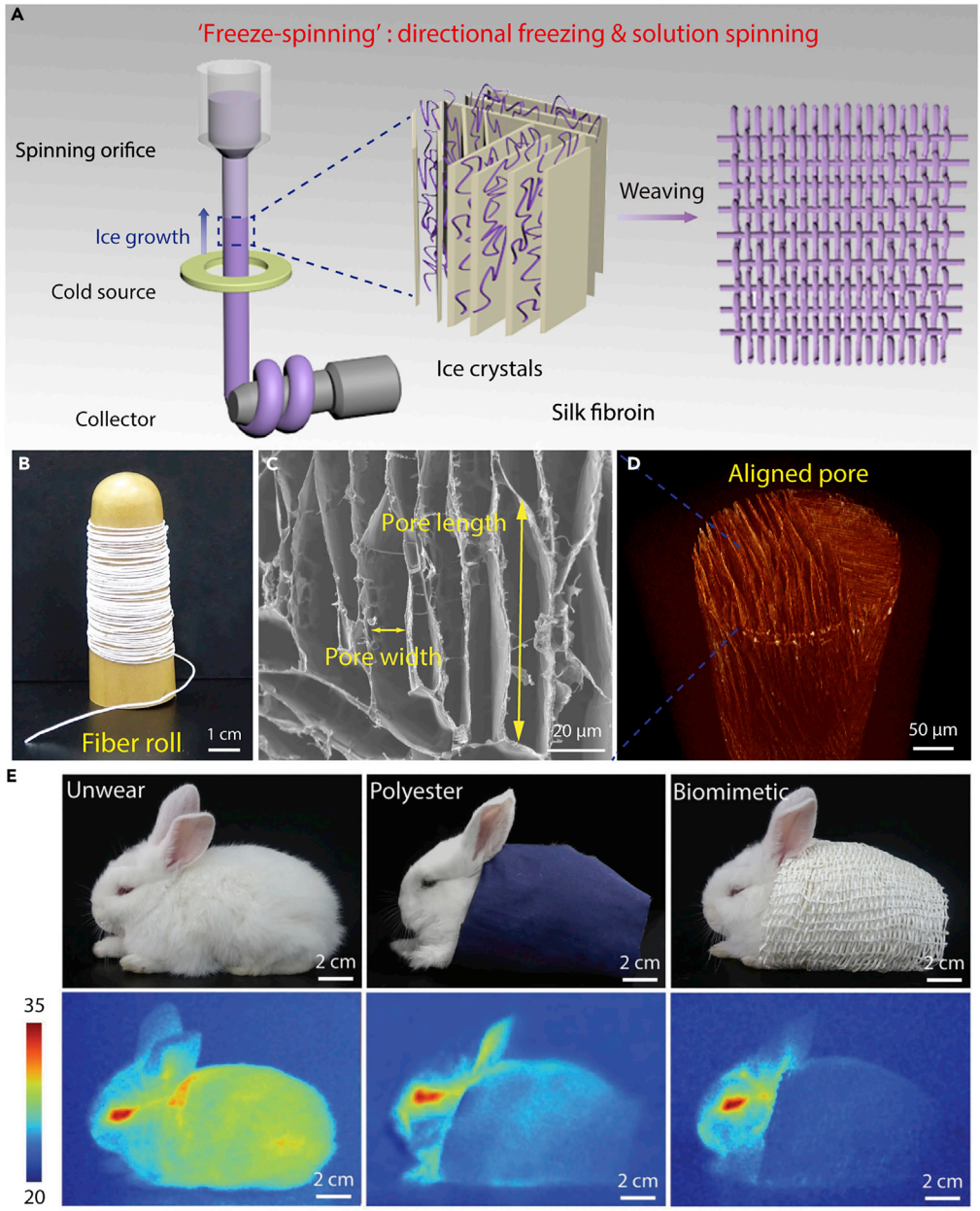

Figure 10. The fabrication, structure, and thermal insulation property of biomimetic porous fibers

(A) Schematic illustration of the "freeze-spinning" technique.

(B) Optical image showing a porous fiber collected in a roll.

(C) Radial cross-sectional SEM image showing the typical structure of a biomimetic porous fiber.

(D) X-ray computed microtomography image showing the aligned lamellar pores within the biomimetic fiber along its axial direction.

(E) Optical and infrared image of a rabbit before and after wearing different textiles showing the remarkable thermal stealth property of the biomimetic porous fiber. Adapted with permission from Cui et al. (2018). Copyright 2018, Wiley-VCH.

combining "directional freezing" and "solution spinning" processes (Figure 10) (Cui et al., 2018), where the extruded silk fibroin solution passed through a cold copper ring and formed a frozen fiber. As the ice crystals grew directionally and preferentially into a lamellar pattern during the freezing process, the resultant freeze-dried fiber possessed aligned lamellar pores along its axis. Silk fibroin was selected in this study due to its favorable processability and good biocompatibility, and the woven textile of biomimetic fibers

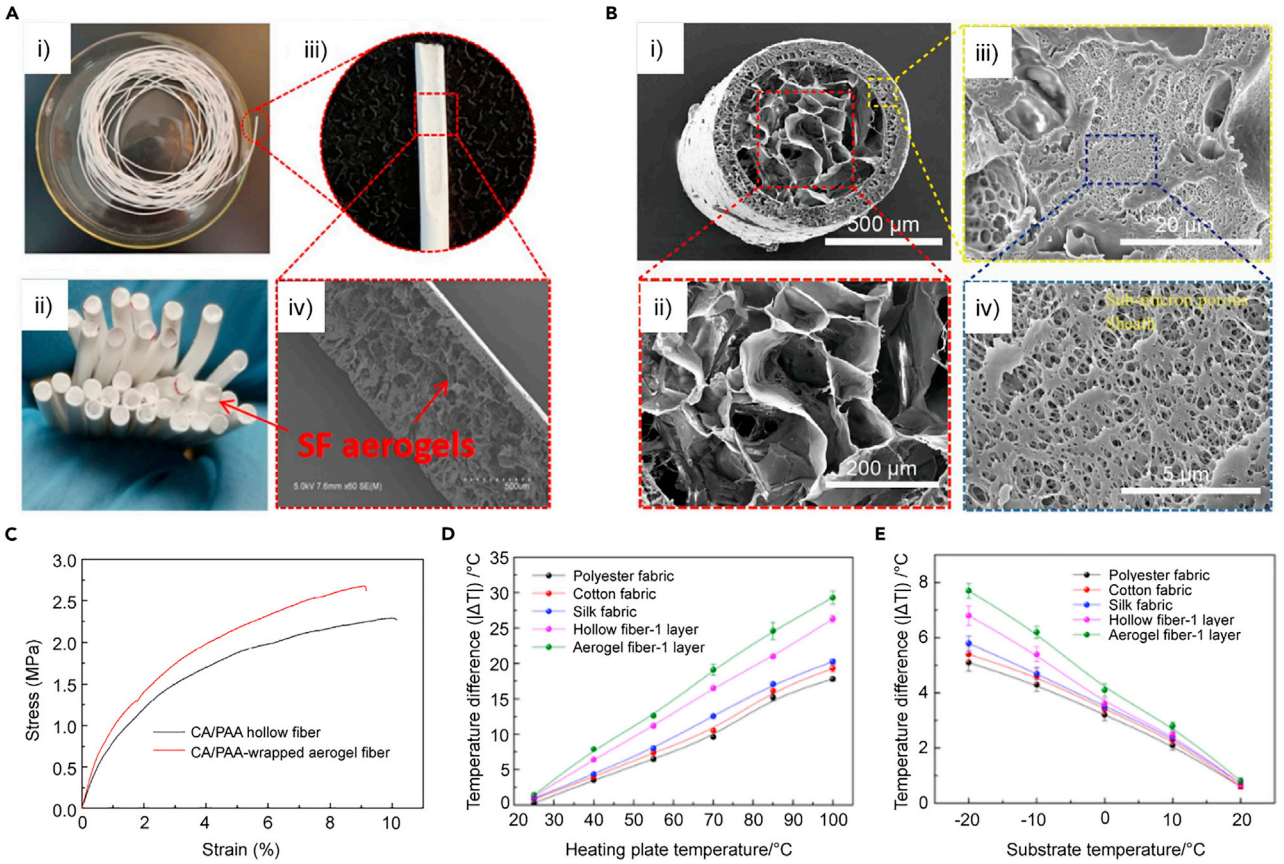

Figure 11. The morphology, microstructure, and properties of porous silk-based aerogel fibers

(A) The CA/PAA-wrapped silk fibroin aerogel fibers with arrows pointing at the exposed aerogel core of aerogel fiber cross-sections.

(B) Cross-sectional SEM images showing the porous sheath and core of a typical fiber.

(C) Stress–strain curves of CA/PAA hollow fiber and CA/PAA-wrapped silk fibroin aerogel fiber.

(D) Temperature difference (|ΔT|) showing the best thermal insulation property of the silk-based aerogel fibers under a simulative hot condition.

(E) |ΔT| showing the best thermal insulation property of the silk-based aerogel fibers under a simulative cold condition. Adapted under the terms and conditions of CC BY license. Yang et al. (2019a). Copyright 2019, The Authors, Published by MDPI.

showed good wearability as well. Benefiting from the porous microstructure (up to 87% porosity) to capture air, such biomimetic textiles had excellent thermal insulation property, superior to commercial silk, cotton, and polyester textiles, indicating efficient personal thermal management applications. More interestingly, the biomimetic textile could be developed into thermal stealth materials, as evidenced by the infrared images where a rabbit body wearing the biomimetic textile became almost invisible regardless of the background temperature.

Aiming at finely mimicking polar bear hair's core-shell structures and improving the mechanical properties of silk-based porous fibers, Yang et al. proposed a step-by-step method (Figure 11) (Yang et al., 2019a). Firstly, a cellulose acetate/polyacrylic acid (CA/PAA) hollow fiber was prepared using coaxial wet spinning, in which the core was filled with water at the beginning and then removed by freeze-drying. Afterwards, silk aqueous solution was injected into the freeze-dried CA/PAA hollow fibers, and rerun the freeze-drying procedure. Finally, the polar-bear-hair-like fiber was successfully constructed, with porous silk fibroin aerogel acting as core and CA/PAA as shell. This biomimetic composite fiber exhibited a high porosity of 86%, and a tensile strength of 2.6 ± 0.4 MPa, which was 3–5 times that of the above fiber without shells (0.57–0.95 MPa). Because the CA/PAA shell went through phase inversion during the first preparation step, both its inner and outer surfaces showed nanoporous structures. Integrated with the silk fibroin aerogel core's micropores, the multiscale porous structures endowed this biomimetic composite fiber with excellent thermal insulation properties in both cold (−20°C) and hot (100°C) conditions.

In addition to the insulating effects dominated by the porous structures of biomimetic fibers, carbon materials could be further incorporated into such silk-based systems for obtaining active heating capability with carbon nanotubes (Cui et al., 2018), or enhancing the infrared radiative heating properties with graphene oxide (Wang et al., 2020b). These products would be well applied in personal thermal management, and more importantly, they lighted the way for the fabrication of multi-functionalized biomimetic fibers beyond the natural inspirations.

CONCLUSION AND OUTLOOKS

The excellent mechanical properties, favorable versatility, and good biocompatibility render silk a very promising raw material for constructing high-performance biomimetic materials. In this review, silk-based structural and functional materials inspired by some typical natural biological materials including bone, nacre, skin, and polar bear hairs, are thoroughly displayed and discussed. It should be noted that the bionic systems are certainly not limited to the above-mentioned ones, as silk fiber itself is also a classic example to be extensively imitated (Ling et al., 2017b). Given that several good review articles had systematically summarized the development of bioinspired spinning and regenerated silk fibers (Koeppel and Holland, 2017; Liu et al., 2019b; Shang et al., 2019), we herein do not mainly focus on this subject. But in respect to expanding raw material sources, those artificial silk fibers prepared from waste silk, or those with mechanical performance superior to native silk, will make a considerable contribution.

Despite the progress achieved in silk-based bioinspired materials during the past decades, there are still challenges for their structural design and bulk production. Indeed, it is hard to completely replicate the full-scale hierarchical architectures of natural biological materials at ambient conditions. To this end, we try to propose a viewpoint combining reductionism and integratism. Specifically, reductionism requires us to perfectly analyze the composition and structure of biological materials from macroscale to nanoscale. For example, Reznikov et al.'s 3D observation and characterization resulted in an expansion of the previously known hierarchical structure of bone to at least 12 levels (Reznikov et al., 2018), with particularly elucidating the organization and relationship between bone's principal components—mineral and collagen, which will definitely help to understand the delicate design of bone in every single detail. Integratism, generally speaking, reminds us to use identical or similar components to build biomimetic materials, with emphasizing on the integration of the multiple components or multiscale structures. For example, Mao et al. fabricated a millimeter-thick synthetic nacre that highly resembles both the chemical composition and the hierarchical structure of natural nacre (Mao et al., 2016). This was achieved by an "assembly-and-mineralization" approach inspired by the natural process in mollusks, where silk fibroin formed the organic layers between the aragonite layers and played a vital role for adhesion. In this regard, will it be a better alternative using catechol-groups-modified silk molecules (Burke et al., 2016) with improved adhesive capability? The answer is unknown. Whereas, in terms of bone-like composites, genetically engineered silk protein fused with HAP-binding domain VTKHLNQISQSY (VTK) had been confirmed to promote biomineralization and thus further enhanced osteoinductivity (Dinjaski et al., 2017). In addition, the inherent arginine–glycine–aspartate (RGD) motif existed in some wild silk could induce cell attachment and proliferation in bone tissue engineering (Behera et al., 2017; Sahu et al., 2015). Hence, taking full advantage of silk by directional selection or optimization of its features may provide a solid material foundation for the future silk-based bioinspired functional composites.

With challenges remaining for building high-performance bioinspired materials in practical form and in bulk, a systematic methodology for dealing with the structural complexity of a truly bioinspired structure whose dimensions span from the nanoscale to the macroscale is highly demanded for scientists and engineers, while combining two or more fabrication technologies may work out as a solution (Wegst et al., 2015). Certainly, the development of silk-based bioinspired structural and functional materials will also follow this route. Hopefully, there will be a breakthrough in the near future.

ACKNOWLEDGMENTS

This work was financially supported by the National Key Research and Development Program of China (No. 2017YFC1103900), the National Natural Science Foundation of China (Nos. 52103149, 51873191, 22075244, 51722306 and 21674098), 2020 Talent Cultivation Project of Zhejiang Association for Science and Technology (CTZB-2020080127-18), the State Key Laboratory of Chemical Engineering (Grant No. SKL-ChE-20T06), and Zhejiang University start-up fund.

AUTHOR CONTRIBUTIONS

Z.X., W.G., and H.B. conceived the idea and designed the frame. Z.X. wrote the draft of the manuscript. W.G. and H.B. revised the manuscript.

DECLARATION OF INTERESTS

The authors declare no competing interests.

REFERENCES

Aigner, T.B., DeSimone, E., and Scheibel, T. (2018). Biomedical applications of recombinant silk-based materials. Adv. Mater. *30*, e1704636.

Bai, H., Walsh, F., Gludovatz, B., Delattre, B., Huang, C., Chen, Y., Tomsia, A.P., and Ritchie, R.O. (2016). Bioinspired hydroxyapatite/poly(methyl methacrylate) composite with a nacre-mimetic architecture by a bidirectional freezing method. Adv. Mater. *28*, 50–56.

Bandar Abadi, M., Weissing, R., Wilhelm, M., Demidov, Y., Auer, J., Ghazanfari, S., Anasori, B., Mathur, S., and Maleki, H. (2021). Nacre-mimetic, mechanically flexible, and electrically conductive silk fibroin-MXene composite foams as piezoresistive pressure sensors. ACS Appl. Mater. Interfaces *13*, 34996–35007.

Barthelat, F., Yin, Z., and Buehler, M.J. (2016). Structure and mechanics of interfaces in biological materials. Nat. Rev. Mater. *1*, 16007.

Behera, S., Naskar, D., Sapru, S., Bhattacharjee, P., Dey, T., Ghosh, A.K., Mandal, M., and Kundu, S.C. (2017). Hydroxyapatite reinforced inherent RGD containing silk fibroin composite scaffolds: promising platform for bone tissue engineering. Nanomedicine *13*, 1745–1759.

Bhattacharjee, P., Kundu, B., Naskar, D., Kim, H.W., Maiti, T.K., Bhattacharya, D., and Kundu, S.C. (2017). Silk scaffolds in bone tissue engineering: an overview. Acta Biomater. *63*, 1–17.

Burke, K.A., Roberts, D.C., and Kaplan, D.L. (2016). Silk fibroin aqueous-based adhesives inspired by mussel adhesive proteins. Biomacromolecules *17*, 237–245.

Chen, F., Porter, D., and Vollrath, F. (2012). Morphology and structure of silkworm cocoons. Mater. Sci. Eng. C *32*, 772–778.

Chen, J., Xin, W., Kong, X., Qian, Y., Zhao, X., Chen, W., Sun, Y., Wu, Y., Jiang, L., and Wen, L. (2020). Ultrathin and robust silk fibroin membrane for high-performance osmotic energy conversion. ACS Energy Lett *5*, 742–748.

Chortos, A., and Bao, Z. (2014). Skin-inspired electronic devices. Mater. Today *17*, 321–331.

Collins, A.M., Skaer, N.J.V., Gheysens, T., Knight, D., Bertram, C., Roach, H.I., Oreffo, R.O.C., Von-Aulock, S., Baris, T., Skinner, J., et al. (2009). Bone-like resorbable silk-based scaffolds for load-bearing osteoregenerative applications. Adv. Mater. *21*, 75–78.

Cui, Y., Gong, H., Wang, Y., Li, D., and Bai, H. (2018). A thermally insulating textile inspired by polar bear hair. Adv. Mater. *30*, e1706807.

Dinjaski, N., Plowright, R., Zhou, S., Belton, D.J., Perry, C.C., and Kaplan, D.L. (2017). Osteoinductive recombinant silk fusion proteins for bone regeneration. Acta Biomater. *49*, 127–139.

Du, G., Mao, A., Yu, J., Hou, J., Zhao, N., Han, J., Zhao, Q., Gao, W., Xie, T., and Bai, H. (2019a). Nacre-mimetic composite with intrinsic self-healing and shape-programming capability. Nat. Commun. *10*, 800.

Du, H., Steiner, U., and Amstad, E. (2019b). Nacre-inspired hard and tough materials. Chimia (Aarau) *73*, 29–34.

Eder, M., Amini, S., and Fratzl, P. (2018). Biological composites—complex structures for functional diversity. Science *362*, 543–547.

Farokhi, M., Mottaghitalab, F., Samani, S., Shokrgozar, M.A., Kundu, S.C., Reis, R.L., Fatahi, Y., and Kaplan, D.L. (2018). Silk fibroin/hydroxyapatite composites for bone tissue engineering. Biotechnol. Adv. *36*, 68–91.

Fitzpatrick, V., Martin-Moldes, Z., Deck, A., Torres-Sanchez, R., Valat, A., Cairns, D., Li, C., and Kaplan, D.L. (2021). Functionalized 3D-printed silk-hydroxyapatite scaffolds for enhanced bone regeneration with innervation and vascularization. Biomaterials *276*, 120995.

Fu, C., Porter, D., Chen, X., Vollrath, F., and Shao, Z. (2011). Understanding the mechanical properties of *Antheraea Pernyi* silk-from primary structure to condensed structure of the protein. Adv. Funct. Mater. *21*, 729–737.

Fu, C., Wang, Y., Guan, J., Chen, X., Vollrath, F., and Shao, Z. (2019). Cryogenic toughness of natural silk and a proposed structure–function relationship. Mater. Chem. Front. *3*, 2507–2513.

Gao, W., Wang, M., and Bai, H. (2020). A review of multifunctional nacre-mimetic materials based on bidirectional freeze casting. J. Mech. Behav. Biomed. Mater. *109*, 103820.

Gerhard, E.M., Wang, W., Li, C., Guo, J., Ozbolat, I.T., Rahn, K.M., Armstrong, A.D., Xia, J., Qian, G., and Yang, J. (2017). Design strategies and applications of nacre-based biomaterials. Acta Biomater. *54*, 21–34.

Geyer, R., Jambeck, J.R., and Law, K.L. (2017). Production, use, and fate of all plastics ever made. Sci. Adv. *3*, e1700782.

Guan, Q.-F., Yang, H.-B., Han, Z.-M., Zhou, L.-C., Zhu, Y.-B., Ling, Z.-C., Jiang, H.-B., Wang, P.-F., Ma, T., Wu, H.-A., et al. (2020). Lightweight, tough, and sustainable cellulose nanofiber-derived bulk structural materials with low thermal expansion coefficient. Sci. Adv. *6*, eaaz1114.

Guo, C., Li, C., Vu, H.V., Hanna, P., Lechtig, A., Qiu, Y., Mu, X., Ling, S., Nazarian, A., Lin, S.J., et al. (2020). Thermoplastic moulding of regenerated silk. Nat. Mater. *19*, 102–108.

Han, J., Du, G., Gao, W., and Bai, H. (2019). An anisotropically high thermal conductive boron nitride/epoxy composite based on nacre-mimetic 3D network. Adv. Funct. Mater. *29*, 1900412.

Ho, M.-p., Wang, H., and Lau, K.-t. (2012). Effect of degumming time on silkworm silk fibre for biodegradable polymer composites. Appl. Surf. Sci. *258*, 3948–3955.

Holland, C., Numata, K., Rnjak-Kovacina, J., and Seib, F.P. (2019). The biomedical use of silk: past, present, future. Adv. Healthc. Mater. *8*, e1800465.

Humenik, M., Lang, G., and Scheibel, T. (2018). Silk nanofibril self-assembly versus electrospinning. Wiley Interdiscip. Rev. Nanomed Nanobiotechnol. *10*, e1509.

Hu, X., Shmelev, K., Sun, L., Gil, E.S., Park, S.H., Cebe, P., and Kaplan, D.L. (2011). Regulation of silk material structure by temperature-controlled water vapor annealing. Biomacromolecules *12*, 1686–1696.

Jambeck, J.R., Geyer, R., Wilcox, C., Siegler, T.R., Perryman, M., Andrady, A., Narayan, R., and Law, K.L. (2015). Plastic waste inputs from land into the ocean. Science *347*, 768–771.

Jin, Y., Kundu, B., Cai, Y., Kundu, S.C., and Yao, J. (2015). Bio-inspired mineralization of hydroxyapatite in 3D silk fibroin hydrogel for bone tissue engineering. Colloid Surf. B Biointerfaces *134*, 339–345.

Koeppel, A., and Holland, C. (2017). Progress and trends in artificial silk spinning: a systematic review. ACS Biomater. Sci. Eng. *3*, 226–237.

Koh, L.D., Cheng, Y., Teng, C.P., and Khin, Y.W. (2015). Structures, mechanical properties and applications of silk fibroin materials. Prog. Polym. Sci. *46*, 86–110.

Kundu, B., Rajkhowa, R., Kundu, S.C., and Wang, X. (2013). Silk fibroin biomaterials for tissue regenerations. Adv. Drug Deliv. Rev. *65*, 457–470.

Li, C., Wu, J., Shi, H., Xia, Z., Sahoo, J.K., Yeo, J., and Kaplan, D.L. (2021). Fiber-based biopolymer processing as a route toward sustainability. Adv. Mater. *34*, e2105196.

Li, D., Bu, X., Xu, Z., Luo, Y., and Bai, H. (2020a). Bioinspired multifunctional cellular plastics with a negative Poisson's ratio for high-energy dissipation. Adv. Mater. *32*, 2001222.

Li, G., Li, Y., Chen, G., He, J., Han, Y., Wang, X., and Kaplan, D.L. (2015). Silk-based biomaterials in biomedical textiles and fiber-based implants. Adv. Healthc. Mater. *4*, 1134–1151.

Li, L., Liang, Y., Wang, G., Xu, P., Yang, L., Hou, S., Zhou, J., Wang, L., Li, X., Yang, L., et al. (2020b). In vivo disintegration and bioresorption of a nacre-inspired graphene-silk film caused by the foreign-body reaction. iScience *23*, 101155.

Ling, S., Jin, K., Kaplan, D.L., and Buehler, M.J. (2016a). Ultrathin free-standing *Bombyx mori* silk nanofibril membranes. Nano Lett. *16*, 3795–3800.

Ling, S., Jin, K., Qin, Z., Li, C., Zheng, K., Zhao, Y., Wang, Q., Kaplan, D.L., and Buehler, M.J. (2018a). Combining in silico design and biomimetic assembly: a new approach for developing high-performance dynamic responsive bio-nanomaterials. Adv. Mater. *30*, e1802306.

Ling, S., Kaplan, D.L., and Buehler, M.J. (2018b). Nanofibrils in nature and materials engineering. Nat. Rev. Mater. *3*, 18016.

Ling, S., Li, C., Jin, K., Kaplan, D.L., and Buehler, M.J. (2016b). Liquid exfoliated natural silk nanofibrils: applications in optical and electrical devices. Adv. Mater. *28*, 7783–7790.

Ling, S., Qin, Z., Huang, W., Cao, S., Kaplan, D.L., and Buehler, M.J. (2017a). Design and function of biomimetic multilayer water purification membranes. Sci. Adv. *3*, e1601939.

Ling, S., Qin, Z., Li, C., Huang, W., Kaplan, D.L., and Buehler, M.J. (2017b). Polymorphic regenerated silk fibers assembled through bioinspired spinning. Nat. Commun. *8*, 1387.

Liu, K., Jiang, Y., Bao, Z., and Yan, X. (2019a). Skin-inspired electronics enabled by supramolecular polymeric materials. CCS Chem. *1*, 431–447.

Liu, Y., Ren, J., and Ling, S. (2019b). Bioinspired and biomimetic silk spinning. Compos. Commun. *13*, 85–96.

Long, D., Cheng, X., Hao, Z., Sun, J., Umuhoza, D., Liu, Y., Chen, L., Xiang, Z., Yang, F., and Zhao, A. (2021). Genetic hybridization of highly active exogenous functional proteins into silk-based materials using "light-clothing" strategy. Matter *4*, 2039–2058.

Mao, A., Zhao, N., Liang, Y., and Bai, H. (2021). Mechanically efficient cellular materials inspired by cuttlebone. Adv. Mater. *33*, 2007348.

Mao, L.-B., Gao, H.-L., Yao, H.-B., Liu, L., Cölfen, H., Liu, G., Chen, S.-M., Li, S.-K., Yan, Y.-X., Liu, Y.-Y., et al. (2016). Synthetic nacre by predesigned matrix-directed mineralization. Science *354*, 107–110.

Melke, J., Midha, S., Ghosh, S., Ito, K., and Hofmann, S. (2016). Silk fibroin as biomaterial for bone tissue engineering. Acta Biomater. *31*, 1–16.

Meyers, M.A., McKittrick, J., and Chen, P.-Y. (2013). Structural biological materials: critical mechanics-materials connections. Science *339*, 773–779.

Mohanty, A.K., Vivekanandhan, S., Pin, J.-M., and Misra, M. (2018). Composites from renewable and sustainable resources: challenges and innovations. Science *362*, 536–542.

Murphy, A.R., and Kaplan, D.L. (2009). Biomedical applications of chemically-modified silk fibroin. J. Mater. Chem. *19*, 6443–6450.

Ni Annaidh, A., Bruyere, K., Destrade, M., Gilchrist, M.D., and Ottenio, M. (2012). Characterization of the anisotropic mechanical properties of excised human skin. J. Mech. Behav. Biomed. Mater. *5*, 139–148.

Omenetto, F.G., and Kaplan, D.L. (2010). New opportunities for an ancient material. Science *329*, 528–531.

Pan, X.F., Wu, B., Gao, H.L., Chen, S.M., Zhu, Y., Zhou, L., Wu, H., and Yu, S.H. (2021). Double-layer nacre-inspired polyimide-mica nanocomposite films with excellent mechanical stability for LEO environmental conditions. Adv. Mater. *34*, e2105299.

Reznikov, N., Bilton, M., Lari, L., Stevens, M.M., and Kroger, R. (2018). Fractal-like hierarchical organization of bone begins at the nanoscale. Science *360*, eaao2189.

Rockwood, D.N., Preda, R.C., Yucel, T., Wang, X., Lovett, M.L., and Kaplan, D.L. (2011). Materials fabrication from *Bombyx mori* silk fibroin. Nat. Protoc. *6*, 1612–1631.

Sahu, N., Baligar, P., Midha, S., Kundu, B., Bhattacharjee, M., Mukherjee, S., Mukherjee, S., Maushart, F., Das, S., Loparic, M., et al. (2015). Nonmulberry silk fibroin scaffold shows superior osteoconductivity than mulberry silk fibroin in calvarial bone regeneration. Adv. Healthc. Mater. *4*, 1709–1721.

Saleem, M., Rasheed, S., and Yougen, C. (2020). Silk fibroin/hydroxyapatite scaffold: a highly compatible material for bone regeneration. Sci. Technol. Adv. Mater. *21*, 242–266.

Scheller, J., Gührs, K., Grosse, F., and Conrad, U. (2001). Production of spider silk proteins in tobacco and potato. Nat. Biotechnol. *19*, 573–577.

Shah, D.U., Porter, D., and Vollrath, F. (2014). Can silk become an effective reinforcing fibre? A property comparison with flax and glass reinforced composites. Compos. Sci. Technol. *101*, 173–183.

Shang, L., Yu, Y., Liu, Y., Chen, Z., Kong, T., and Zhao, Y. (2019). Spinning and applications of bioinspired fiber systems. ACS Nano *13*, 2749–2772.

Shao, Z., and Vollrath, F. (2002). Surprising strength of silkworm silk. Nature *418*, 741.

Shao, Z., Wang, Y., and Bai, H. (2020). A superhydrophobic textile inspired by polar bear hair for both in air and underwater thermal insulation. Chem. Eng. J. *397*, 125441.

Shi, C., Hu, F., Wu, R., Xu, Z., Shao, G., Yu, R., and Liu, X.Y. (2021). New silk road: from mesoscopic reconstruction/functionalization to flexible meso-electronics/photonics based on cocoon silk materials. Adv. Mater. *33*, e2005910.

Tao, H., Kaplan, D.L., and Omenetto, F.G. (2012). Silk materials–A road to sustainable high technology. Adv. Mater. *24*, 2824–2837.

Teule, F., Miao, Y.G., Sohn, B.H., Kim, Y.S., Hull, J.J., Fraser, M.J., Jr., Lewis, R.V., and Jarvis, D.L. (2012). Silkworms transformed with chimeric silkworm/spider silk genes spin composite silk fibers with improved mechanical properties. Proc. Natl. Acad. Sci. U S A *109*, 923–928.

Ude, A.U., Eshkoor, R.A., Zulkifili, R., Ariffin, A.K., Dzuraidah, A.W., and Azhari, C.H. (2014). *Bombyx mori* silk fibre and its composite: a review of contemporary developments. Mater. Des. *57*, 298–305.

Wang, C., Xia, K., Zhang, Y., and Kaplan, D.L. (2019a). Silk-based advanced materials for soft electronics. Acc. Chem. Res. *52*, 2916–2927.

Wang, C., Yokota, T., and Someya, T. (2021a). Natural biopolymer-based biocompatible conductors for stretchable bioelectronics. Chem. Rev. *121*, 2109–2146.

Wang, C., Zhu, M., Yu, H.Y., Abdalkarim, S.Y.H., Ouyang, Z., Zhu, J., and Yao, J. (2021b). Multifunctional biosensors made with self-healable silk fibroin imitating skin. ACS Appl. Mater. Interfaces *13*, 33371–33382.

Wang, Q., Ling, S., Liang, X., Wang, H., Lu, H., and Zhang, Y. (2019b). Self-healable multifunctional electronic tattoos based on silk and graphene. Adv. Funct. Mater. *29*, 1808695.

Wang, Q., Zhang, Y., Li, B., and Chen, L. (2017). Controlled dual delivery of low doses of BMP-2 and VEGF in a silk fibroin-nanohydroxyapatite scaffold for vascularized bone regeneration. J. Mater. Chem. B *5*, 6963–6972.

Wang, Y., Cui, Y., Shao, Z., Gao, W., Fan, W., Liu, T., and Bai, H. (2020a). Multifunctional polyimide aerogel textile inspired by polar bear hair for thermoregulation in extreme environments. Chem. Eng. J. *390*, 124623.

Wang, Y., Ma, R., Hu, K., Kim, S., Fang, G., Shao, Z., and Tsukruk, V.V. (2016). Dramatic enhancement of graphene oxide/silk nanocomposite membranes: increasing toughness, strength, and Young's modulus via annealing of interfacial structures. ACS Appl. Mater. Interfaces *8*, 24962–24973.

Wang, Z., Yang, H., Li, Y., and Zheng, X. (2020b). Robust silk fibroin/graphene oxide aerogel fiber for radiative heating textiles. ACS Appl. Mater. Interfaces *12*, 15726–15736.

Wegst, U.G., Bai, H., Saiz, E., Tomsia, A.P., and Ritchie, R.O. (2015). Bioinspired structural materials. Nat. Mater. *14*, 23–36.

Wenk, E., Merkle, H.P., and Meinel, L. (2011). Silk fibroin as a vehicle for drug delivery applications. J. Contro. Release *150*, 128–141.

Whittall, D.R., Baker, K.V., Breitling, R., and Takano, E. (2021). Host systems for the production of recombinant spider silk. Trends Biotechnol. *39*, 560–573.

Xin, W., Lin, C., Fu, L., Kong, X.Y., Yang, L., Qian, Y., Zhu, C., Zhang, Q., Jiang, L., and Wen, L. (2021). Nacre-like mechanically robust heterojunction for lithium-ion extraction. Matter *4*, 737–754.

Xin, W., Xiao, H., Kong, X.Y., Chen, J., Yang, L., Niu, B., Qian, Y., Teng, Y., Jiang, L., and Wen, L.

(2020). Biomimetic nacre-like silk-crosslinked membranes for osmotic energy harvesting. ACS Nano *14*, 9701–9710.

Xin, W., Zhang, Z., Huang, X., Hu, Y., Zhou, T., Zhu, C., Kong, X.Y., Jiang, L., and Wen, L. (2019). High-performance silk-based hybrid membranes employed for osmotic energy conversion. Nat. Commun. *10*, 3876.

Xu, Z., Shi, L., Yang, M., Zhang, H., and Zhu, L. (2015). Fabrication of a novel blended membrane with chitosan and silk microfibers for wound healing: characterization, in vitro and in vivo studies. J. Mater. Chem. B *3*, 3634–3642.

Xu, Z., Shi, L., Yang, M., and Zhu, L. (2019). Preparation and biomedical applications of silk fibroin-nanoparticles composites with enhanced properties - a review. Mater. Sci. Eng. C Mater. Biol. Appl. *95*, 302–311.

Xu, Z., Wu, M., Gao, W., and Bai, H. (2020). A transparent, skin-inspired composite film with outstanding tear resistance based on flat silk cocoon. Adv. Mater. *32*, e2002695.

Yang, H., Wang, Z., Liu, Z., Cheng, H., and Li, C. (2019a). Continuous, strong, porous silk firoin-based aerogel fibers toward textile thermal insulation. Polymers (Basel) *11*, 1899.

Yang, H., Wang, Z., Wang, M., and Li, C. (2020). Structure and properties of silk fibroin aerogels prepared by non-alkali degumming process. Polymer *192*, 122298.

Yang, K., Guan, J., Numata, K., Wu, C., Wu, S., Shao, Z., and Ritchie, R.O. (2019b). Integrating tough *Antheraea pernyi* silk and strong carbon fibres for impact-critical structural composites. Nat. Commun. *10*, 3786.

Yang, W., Sherman, V.R., Gludovatz, B., Schaible, E., Stewart, P., Ritchie, R.O., and Meyers, M.A. (2015). On the tear resistance of skin. Nat. Commun. *6*, 6649.

Yarger, J.L., Cherry, B.R., and Vaart, A. (2018). Uncovering the structure–function relationship in spider silk. Nat. Rev. Mater. *3*, 18008.

Yu, X., Shou, W., Mahajan, B.K., Huang, X., and Pan, H. (2018). Materials, processes, and facile manufacturing for bioresorbable electronics: a review. Adv. Mater. *30*, e1707624.

Zhao, N., Li, M., Gong, H., and Bai, H. (2020). Controlling ice formation on gradient wettability surface for high-performance bioinspired materials. Sci. Adv. *6*, eabb4712.

Zhao, N., Wang, Z., Cai, C., Shen, H., Liang, F., Wang, D., Wang, C., Zhu, T., Guo, J., Wang, Y., et al. (2014). Bioinspired materials: from low to high dimensional structure. Adv. Mater. *26*, 6994–7017.

Zhu, B., Wang, H., Leow, W.R., Cai, Y., Loh, X.J., Han, M.Y., and Chen, X. (2016). Silk fibroin for flexible electronic devices. Adv. Mater. *28*, 4250–4265.